Transcription factor Lhx2 is necessary and sufficient to suppress astrogliogenesis and promote neurogenesis in the developing hippocampus

Lakshmi Subramanian[a,1], Anindita Sarkar[a,1], Ashwin S. Shetty[a], Bhavana Muralidharan[a], Hari Padmanabhan[a], Michael Piper[b], Edwin S. Monuki[c], Ingolf Bach[d], Richard M. Gronostajski[e,f], Linda J. Richards[b], and Shubha Tole[a,2]

[a]Department of Biological Sciences, Tata Institute of Fundamental Research, Mumbai 400005, India; [b]Queensland Brain Institute and School of Biomedical Sciences, University of Queensland, Brisbane, Queensland 4072, Australia; [c]Department of Pathology and Laboratory Medicine, School of Medicine, University of California, Irvine, CA 92697; [d]Programs in Gene Function and Expression and Molecular Medicine, University of Massachusetts Medical School, Worcester, MA 01605; [e]Department of Biochemistry, State University of New York, Buffalo, NY14203; and [f]Developmental Genomics Group, New York State Center of Excellence in Bioinformatics and Life Sciences, Buffalo, NY 14203

Edited by Clifford J. Tabin, Harvard Medical School, Boston, MA, and approved May 18, 2011 (received for review January 21, 2011)

The sequential production of neurons and astrocytes from neuroepithelial precursors is a fundamental feature of central nervous system development. We report that LIM-homeodomain (LIM-HD) transcription factor Lhx2 regulates this transition in the developing hippocampus. Disrupting Lhx2 function in the embryonic hippocampus by in utero electroporation and in organotypic slice culture caused the premature production of astrocytes at stages when neurons are normally generated. Lhx2 function is therefore necessary to suppress astrogliogenesis during the neurogenic period. Furthermore, Lhx2 overexpression was sufficient to suppress astrogliogenesis and prolong the neurogenic period. We provide evidence that Lhx2 overexpression can counteract the instructive astrogliogenic effect of Notch activation. Lhx2 overexpression was also able to override and suppress the activation of the GFAP promoter by Nfia, a Notch-regulated transcription factor that is required for gliogenesis. Thus, Lhx2 appears to act as a "brake" on Notch/Nfia-mediated astrogliogenesis. This critical role for Lhx2 is spatially restricted to the hippocampus, because loss of Lhx2 function in the neocortex did not result in premature astrogliogenesis at the expense of neurogenesis. Our results therefore place Lhx2 as a central regulator of the neuron-glia cell fate decision in the hippocampus and reveal a striking regional specificity of this fundamental function within the dorsal telencephalon.

During the development of the vertebrate CNS, progenitors in the early proliferative neuroepithelium are specified both in terms of their regional identity and in terms of the cell types they will generate. In the telencephalon, LIM-homeodomain (LIM-HD) transcription factor Lhx2 acts as a "selector gene" for cerebral cortical fate. In the absence of Lhx2, the cortical primordium (hippocampus and neocortex) is lost at the expense of alternative noncortical (hem and antihem) fates (1–3). This is an early role for Lhx2, the critical period for which ends at embryonic gestation day (E) 10.5. After this age, loss of Lhx2 does not cause loss of the cortical primordium (3). However, *Lhx2* continues to be expressed in the telencephalic ventricular zone after E10.5 and remains strongly expressed in the hippocampal ventricular zone at midlate gestation stages when hippocampal neurogenesis is underway (4). We tested the hypothesis that Lhx2 may have additional functions in hippocampal progenitors during neurogenesis.

Progenitors throughout the CNS produce neurons as well as astroglia. A characteristic feature of this process, common across all vertebrate species, is that neurogenesis precedes gliogenesis (5). The molecular mechanisms that control this switch in cell fate are not very well understood. However, the Notch signaling pathway is known to play a fundamental role in this process. During the early neurogenic period, the Notch signaling pathway maintains telencephalic progenitors in an undifferentiated state (6). At later stages, however, Notch signaling has a distinct and instructive role in astrogliogenesis (7). In the developing cerebral cortex and spinal cord, Notch signaling activates the transcription factor Nfia, which is necessary and sufficient for astrocytic cell fate (8–11). Although Notch signaling is active from early stages in the telencephalic ventricular zone, astrocytes are not generated during the neurogenic phase. The molecular players that prevent astrocyte specification during the neurogenic period remain unknown.

In this study, we report a unique role for Lhx2 in the hippocampus during the phase of active neurogenesis. We show that loss of Lhx2 produces astrocytes prematurely from progenitors that would otherwise produce neurons. On the other hand, overexpression of Lhx2 enhances and prolongs neurogenesis to generate neurons from progenitors that would otherwise give rise to astrocytes. In the hippocampus, astrogliogenesis can also be prematurely induced by overexpressing constitutively active Notch or its target Nfia. Simultaneous overexpression of full-length Lhx2 can override both of these effects and restore neurogenesis. Lhx2 is able to repress activation of the GFAP promoter, one of the targets of Nfia. Lhx2 therefore acts as a brake on the Notch-Nfia pathway, preventing premature gliogenesis until neurogenesis is complete. Surprisingly, this role of Lhx2 appears to be specific to the hippocampus. In the neocortex, neurons destined for different cortical layers appear to be normally produced despite loss of Lhx2 function in the neocortical progenitors. Our study not only identifies Lhx2 as a key regulator of the neuron-astrocyte cell fate switch in the developing hippocampus but reveals an unexpected spatial selectivity within the telencephalon for this critical function.

Results

Disrupting Lhx2 Function Causes Premature Astrogliogenesis During the Neurogenic Period of Hippocampal Development. We selectively disrupted the *Lhx2* gene using in utero electroporation to introduce Cre recombinase into embryos carrying floxed *Lhx2* [*Lhx2* conditional knockout (*Lhx2* cKO)] (3). Electroporation permits examination of targeted cells in a background of normal cells,

Author contributions: L.S., A.S., H.P., and S.T. designed research; L.S., A.S., A.S.S., B.M., H.P., and M.P. performed research; E.S.M., I.B., R.M.G., and L.J.R. contributed new reagents/analytic tools; L.S., A.S., A.S.S., B.M., H.P., M.P., and S.T. analyzed data; and L.S., A.S., H.P., and S.T. wrote the paper.

The authors declare no conflict of interest.

Freely available online through the PNAS open access option.

This article is a PNAS Direct Submission.

[1]L.S. and A.S. contributed equally to this work.

[2]To whom correspondence should be addressed. E-mail: shubhatole@gmail.com.

See Author Summary on page 10937.

This article contains supporting information online at www.pnas.org/lookup/suppl/doi:10.1073/pnas.1101109108/-/DCSupplemental.

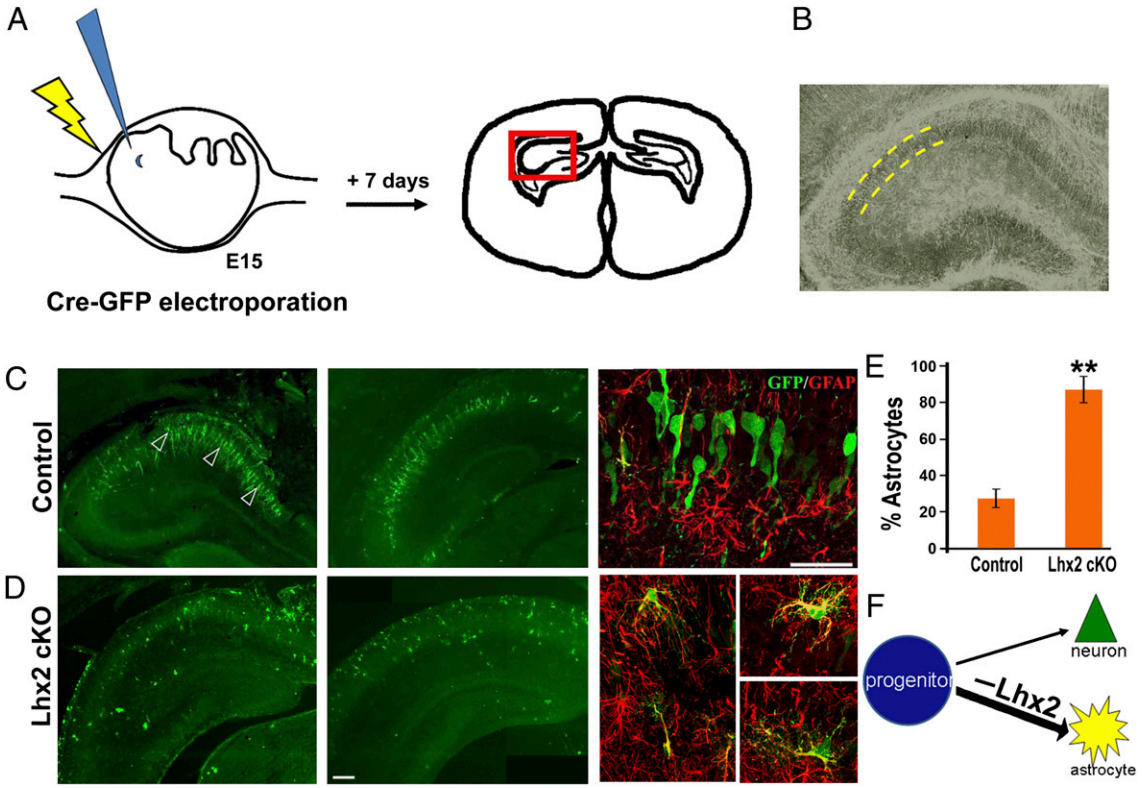

Fig. 1. Lhx2 is necessary for neuronal cell fate in the embryonic hippocampus. (*A*) Schematic of in utero electroporation at E15 and the brain section 7 d after electroporation. (*B*) Phase contrast image of a typical section reveals the densely packed pyramidal cell layer (outlined by yellow dashed lines) in which pyramidal neurons reside. (*C*) In control embryos, electroporation of a Cre-GFP construct labels cells that migrate to the pyramidal cell layer in the hippocampus 7 d after electroporation. These cells display neuronal morphologies and do not show GFAP immunoreactivity (arrowheads). A confocal image of GFP-GFAP labeling is shown alongside the low-magnification montages. (*D*) Electroporation of Cre-GFP into *Lhx2* cKO embryos labels cells scattered within as well as outside the pyramidal cell layer. These cells display multipolar astrocytic morphologies and are GFAP-positive. Confocal images of the GFP-GFAP colocalization are shown alongside the low-magnification montages. (*E*) GFP- and GFAP-expressing cells were scored in electroporated brains. In control embryos electroporated with Cre-GFP, 26% of the GFP-expressing cells were also GFAP-positive. In *Lhx2* cKO embryos, 86% of the GFP-expressing cells were also GFAP-positive. The bars represent the mean ± SD (**$P < 0.0001$). (*F*) Diagram illustrating that loss of Lhx2 in hippocampal progenitors at E15 enhances astrogliogenesis. (Scale bars: 50 μm.) *B* and *D* (second panel) are composites assembled from multiple images.

which is essential to test for cell-autonomous effects. Electroporation also offers the advantage of control of the timing of gene disruption. We selected E14.5 to E15.5, the peak stage of hippocampal neurogenesis, for electroporation (henceforth called E15) and examined the electroporated embryos 6–8 d after electroporation, during early postnatal stages. This is schematized in Fig. 1*A*, and a typical hippocampal section is shown in Fig. 1*B*.

A bicistronic construct encoding Cre recombinase and an EGFP reporter under the CAG promoter was electroporated into *Lhx2* cKO embryos. Littermate embryos carrying a WT allele served as controls. At this stage, the hippocampal ventricular zone is known to produce mainly neurons (12). When examined 7 d later, the majority of GFP-expressing cells in control embryos were found to have assembled into a well-defined pyramidal cell layer, extending arbors characteristic of hippocampal pyramidal neurons and negative for GFAP immunohistochemistry (Fig. 1*C*). In contrast, Cre-GFP electroporation into *Lhx2* cKO embryos resulted in scattered GFP-expressing cells in and around the pyramidal cell layer that coexpressed GFAP. (Fig. 1*D*). A total of 86% of the GFP-expressing cells in *Lhx2* cKO brains expressed GFAP compared with 26% in control brains (Fig. 1*E*). By postnatal stages, the radial glia in the Ammon's horn (CA fields) are greatly reduced; thus, GFAP labeling, together with the position and distinctive morphology of the electroporated cells, is indicative of an astrocytic cell fate (13). Therefore, Lhx2 loss of function appears to promote astrogliogenesis from progenitors that would otherwise have produced hippocampal pyramidal neurons (schematized in Fig. 1*F*).

Dominant-Negative Construct Recapitulates the Lhx2 Loss-of-Function Phenotype. All known functions of LIM-HD proteins that have been investigated at the molecular level require Clim cofactors. Two LIM-HD molecules are bridged by a dimer of Clim proteins to produce the transcriptionally active complex (14) (Fig. 2*B*). A truncated Clim construct lacking the dimerization domain of Clim (ClimΔDD) inhibits the functional activity of LIM-HD proteins, including Lhx2 (15, 16) (Fig. 2*B*). In a pull-down assay, ^{35}S-labeled ClimΔDD binds the LIM domains of Lhx2 protein (Fig. S1). *Lhx2* is the only LIM-HD that is expressed in the entire E15.5 hippocampal ventricular zone. *Lhx9* has a very limited and weak expression (Fig. S1), and *Lhx5* expression is restricted to Cajal–Retzius cells at this stage (17).

We used this construct (ClimΔDD-IRES-EGFP) to perturb Lhx2 function in WT mice. This permitted us to explore the mechanism of Lhx2 function in vivo and in vitro further without being constrained by the availability of *Lhx2* cKO embryos and also allowed us to examine the role of Lhx2 in other mutant strains. WT brains electroporated with the control GFP construct in utero between E14.5 and E15.5 displayed many GFP-labeled cells in a well-ordered arrangement within the pyramidal cell layer 6–8 d after electroporation. These cells showed characteristic hippocampal pyramidal neuronal morphologies and did not express GFAP (Fig. 2*A*). A total of 35% of the GFP-expressing

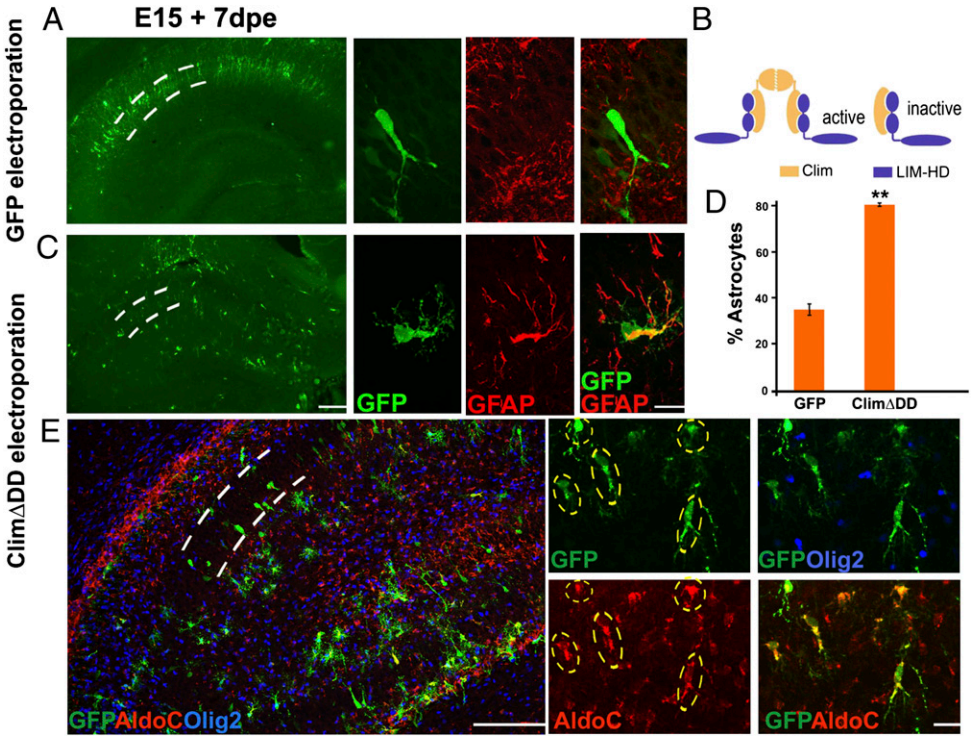

Fig. 2. A dominant-negative construct recapitulates the Lhx2 loss-of-function phenotype. (*A*) WT E15 embryo electroporated with a control GFP construct displays labeled cells in a tightly packed pyramidal cell layer 7 d after electroporation (dashed lines). These cells display characteristic neuronal morphologies and do not express GFAP. Confocal images of GFP-GFAP labeling are shown alongside the low-magnification images. dpe, days postelectroporation. (*B*) Tetrameric model of LIM-HD function illustrating a transcriptionally active complex containing two LIM-HD molecules (blue) and two Clim molecules (yellow). A truncated Clim protein lacking the dimerization domain (ClimΔDD) blocks formation of the tetramer, and thus interferes with LIM-HD protein function. (*C*) Electroporation of ClimΔDD-GFP into WT embryos generates cells scattered throughout the hippocampus, which are GFAP-positive and have multipolar morphologies. Confocal images of GFP-GFAP labeling are shown alongside the low-magnification montages. (*D*) GFP- and GFAP-expressing cells were scored. In embryos electroporated with GFP (controls), 35% of the GFP-expressing cells were also GFAP-positive. In ClimΔDD-GFP electroporated embryos, 80% of the electroporated cells were GFAP-positive. The bars represent the mean ± SD (**$P < 0.001$). (*E*) ClimΔDD-GFP electroporated cells (green cells marked by dashed ovals) express astrocyte-specific marker AldoC (red) but do not express oligodendrocyte marker Olig2 (blue). (Scale bars: low-magnification images, 100 μm; high-magnification images, 20 μm.)

cells were GFAP-positive. In contrast, WT brains electroporated with ClimΔDD displayed electroporated cells scattered in a disorganized manner within and outside the pyramidal cell layer, with irregular morphologies. In these brains, 80% of the GFP-expressing cells were GFAP-positive (Fig. 2*D*). Furthermore, these cells coexpressed Aldolase C (AldoC), a marker of astrocytes, but did not express oligodendrocyte marker Olig2 (18–21) (Fig. 2*E*). In summary, ClimΔDD electroporation promotes astrogliogenesis in progenitors that would otherwise produce neurons. This phenotype was seen in both CA1 and CA3 fields and across all rostrocaudal levels of the hippocampus, similar to the phenotype seen when Cre is electroporated into *Lhx2* cKO brains (Fig. S2). To test whether the astrogliogenic effect we observed may have arisen from effects on cell proliferation or cell death instead of cell fate, we examined control GFP and ClimΔDD electroporated brains 1 d after electroporation. Electroporated cells were still at or near the ventricular zone, and some of them coexpressed proliferation marker Ki67. The proportion of GFP cells that were Ki67-positive was similar in control and ClimΔDD brains. Furthermore, staining for activated caspase 3 showed no enhanced cell death in the experimental brains (Fig. S3). Therefore, interfering with Lhx2 function appears to regulate cell fate per se, apparently without additional effects on progenitor cell proliferation or death.

Overexpression of Lhx2 Enhances and Prolongs Neurogenesis. We tested whether increasing Lhx2 levels in hippocampal progenitors also regulates cell fate. We overexpressed a construct encoding full-length Lhx2 at E15 and analyzed the brains postnatally. Compared with control brains (Fig. 3 *A* and *B*), more cells in Lhx2-overexpressing brains were seen to inhabit the pyramidal cell layer, displaying morphologies appropriate for pyramidal neurons. These cells did not coexpress GFAP (Fig. 3 *C* and *D*). In contrast to the Lhx2 loss of function that dramatically increased astrogliogenesis, overexpression of Lhx2 at E15 caused a significant decrease in the level of astrogliogenesis (35% decreasing to 10%, Fig. 3*I*). Together, these results suggest that Lhx2 promotes neurogenesis by suppressing astrogliogenesis. This raised the possibility that Lhx2 might actively inhibit astrogliogenesis by suppressing gliogenic pathways. To test this idea, we overexpressed Lhx2 at E17, a predominantly gliogenic stage, during which progliogenic pathways are expected to be active. Indeed, control GFP electroporation reveals baseline astrogliogenesis at this stage to be 79%, with electroporated cells showing morphologies and positions appropriate for astrocytes (Fig. 3 *E*, *F*, and *I*). Lhx2 overexpression suppresses gliogenesis and rescues neurogenesis, such that electroporated cells now display pyramidal neuronal morphologies, occupying the pyramidal cell layer in a neat band, and do not express GFAP (Fig. 3 *G* and *H*). Thus, Lhx2 overexpression is able to prolong neurogenesis well into the astrogliogenic period, bringing the level of gliogenesis to 31%, similar to the baseline level at E15 (Fig. 3*I*).

Lhx2 Can Override the Astrogliogenic Effects of Constitutive Notch Activation in Vivo. Notch signaling instructs astrogliogenesis in the embryonic telencephalon (7, 22). Consistent with these studies, we found that constitutive activation of Notch is also a potent

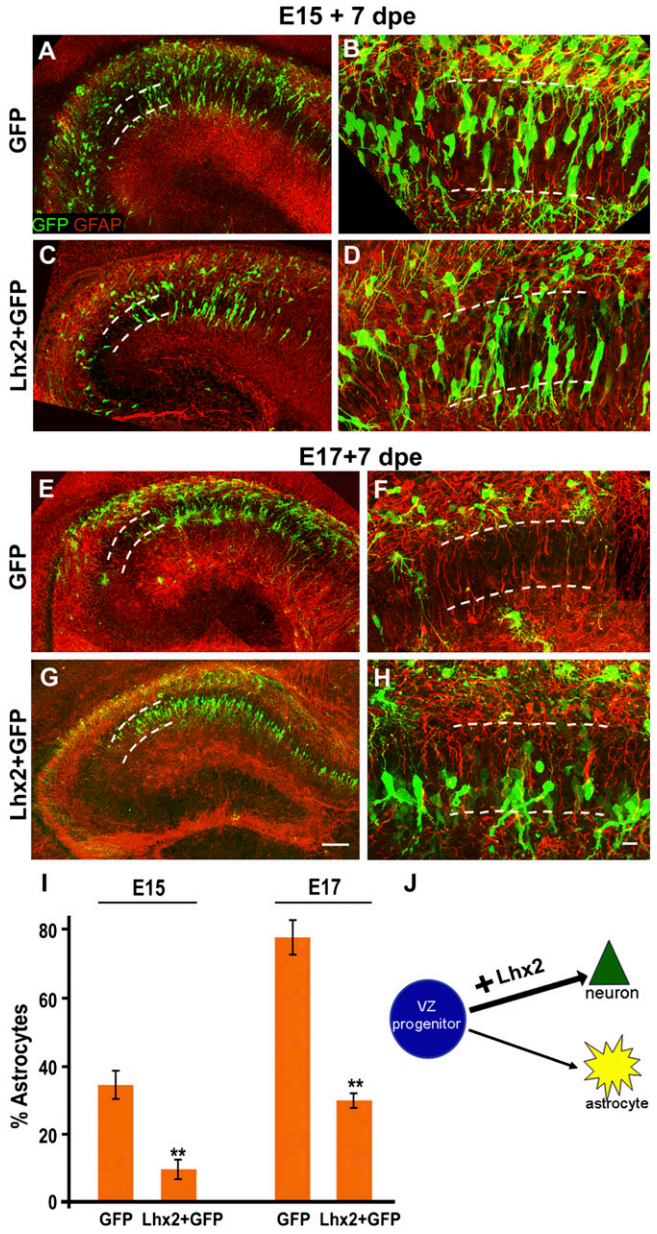

Fig. 3. Lhx2 overexpression enhances and prolongs neurogenesis. (*A* and *B*) WT embryo electroporated with a control GFP construct displays several labeled cells in the pyramidal cell layer 7 d after electroporation (dashed lines). These cells display characteristic neuronal morphologies and do not express GFAP. Other cells are scattered in extrapyramidal locations, and several of them coexpress GFAP. dpe, days postelectroporation. (*C* and *D*) Electroporation of a full-length Lhx2 construct enhances neurogenesis, with fewer cells occupying extrapyramidal positions and expressing GFAP. (*E* and *F*) WT E17 embryo electroporated with a control GFP construct displays labeled cells scattered in extrapyramidal locations 7 d after electroporation (dashed lines). These cells display characteristic astroglial morphologies and coexpress GFAP. The pyramidal layer (dashed lines) appears nearly devoid of GFP cells. (*G* and *H*) Electroporation of a full-length Lhx2 construct enhances neurogenesis, with several cells occupying the pyramidal cell layer in a tight band. These cells display neuronal morphologies and do not coexpress GFAP. (*I*) GFP- and GFAP-expressing cells were scored in electroporated brains. For E15 electroporations, the proportion of GFP cells that were also GFAP-positive in control GFP embryos was 35%, and in Lhx2-overexpressing embryos, the proportion was 10%. In control E17 embryos electroporated with GFP, the proportion was 79%, and in Lhx2-overexpressing embryos, the proportion was 31%. The bars represent the mean ± SD (**$P < 0.0001$). (*J*) Diagram illustrating that Lhx2 overexpression enhances neurogenesis. All high-magnification images are generated from montages of confocal images of GFP (green) and GFAP (red). (Scale bars: low-magnification images, 100 μm; high-magnification images, 20 μm.) *A*–*H* are composites assembled from multiple confocal images.

inducer of astrogliogenesis in the embryonic hippocampus. We overexpressed a construct that encodes a ligand-independent membrane-associated Notch protein (23). When cleaved by endogenous γ-secretase, this protein produces the active Notch intracellular domain fragment (NICD). As expected, coelectroporation of this construct at E15 together with a control GFP construct induced robust astrogliogenesis. When scored 6–8 d after electroporation, GFP-expressing cells took up scattered positions in the hippocampus not limited to the pyramidal cell layer, consistent with the normal localization of astrocytes in the hippocampus (Fig. 4 *A*–*C*). A total of 69% of the GFP-expressing cells coexpressed GFAP. In contrast, when the same NICD construct was coelectroporated with a construct encoding full-length Lhx2-GFP, neurogenesis was partially rescued. Several GFP-expressing cells were now positioned within the pyramidal cell layer, displaying distinctive pyramidal neuronal morphologies and β-tubulin expression (Fig. 4 *D*–*F*). With Lhx2-GFP coelectroporation, the proportion of GFAP-expressing electroporated cells decreased to 51% (Fig. 4*G*). In summary, Lhx2 coelectroporation was able to override Notch-induced astrogliogenesis in a fraction of NICD-expressing cells. This suggested a model in which Lhx2 regulates astrogliogenesis downstream of Notch activation (Fig. 4*H*).

Functional Nfia Is Necessary for Astrogliogenesis Arising from Lhx2 Deprivation. An important target of Notch signaling is the transcription factor Nfia, which is necessary and sufficient for astrogliogenesis (8–11). We sought to test whether Lhx2 loss of function can induce astrogliogenesis in the absence of Nfia. However, *Nfia* mutants die at birth, precluding any such analysis at postnatal stages. Therefore, we set up a combination of ex utero electroporation, followed by an in vitro organotypic explant culture assay. In ex utero electroporation, the brain is dissected out but kept intact and DNA is injected into the ventricle similar to in utero electroporation. Electrodes are applied to the brain as illustrated in the schematic (Fig. 5*A*). This ensures that only cells in the ventricular zone incorporate the DNA, similar to in utero electroporation. The brain is then sectioned coronally, and the hippocampal portion is isolated and maintained as an organotypic slice culture. Hippocampal slice cultures have been used extensively in the literature to examine different aspects of hippocampal development and function (24, 25).

When a control EGFP construct was electroporated, explants displayed axons after 6 d in vitro (Fig. 5*B*). These axons were seen to extend toward the fimbria and encircle the periphery of the explant. This trajectory closely parallels the anatomy of hippocampal projections, which grow parallel to the ventricular surface (corresponding to the periphery of the explant) and exit the hippocampus via the fimbria in vivo. In the explant, axons cannot "exit," and are therefore spread out in the region of the fimbria or encircle the explant. Because the extent of electroporation varies from brain to brain, the numbers of axons per explant could not be scored; however, 100% of the control GFP explants, regardless of extent of electroporation, reliably produced robust fiber bundles (Fig. 5 *C* and *K*). In contrast, electroporation of ClimΔDD resulted in a highly penetrant phenotype, such that none of the explants showed the presence of axons (Fig. 5 *D* and *K*). This phenotype is consistent with the switch to an astrocytic fate observed in vivo and, together with the in utero electroporation data, provides an excellent system to assess the neuron vs. glial fate choice. It also provides an assay to explore the possible interactions of Lhx2 with the gliogenic transcription factor Nfia.

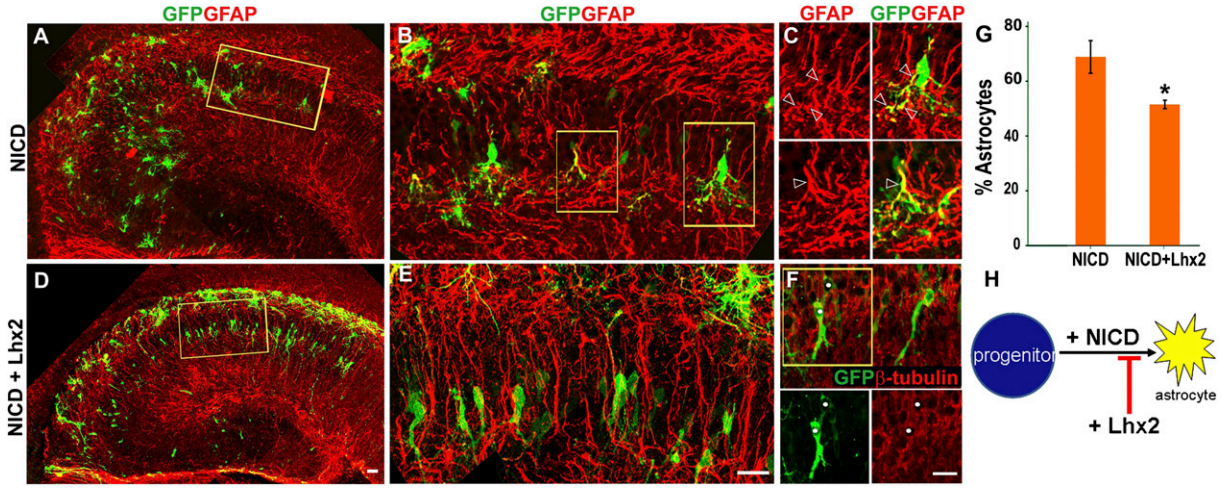

Fig. 4. Lhx2 can override the astrogliogenic effects of constitutive Notch activation in vivo. (*A–C*) Electroporation of a constitutively active Notch construct (NICD) at E15 induces robust astrogliogenesis. Electroporated cells express GFAP and display astrocytic morphologies. A high-magnification confocal image of the boxed area in *A* is shown in *B*. The boxed areas in *B* are shown in *C* as single GFAP (red) and overlay (GFP-GFAP) images. Open arrowheads mark processes of the same cells in each image pair. (*D–F*) Lhx2-GFP coelectroporated with NICD is able to rescue neurogenesis partially. Many electroporated cells do not express GFAP but, instead, express β-tubulin and display pyramidal neuronal morphologies. A high-magnification confocal image of the boxed area in *D* is shown in *E*. *F* shows β-tubulin (red) and GFP (green) image overlays. White circles mark the same cells in each panel. (*G*) GFP-expressing cells were scored. In NICD electroporated brains, 69% of the electroporated cells were GFAP-positive. This number decreased to 51% when NICD was coelectroporated with Lhx2. The bars represent the mean ± SD (*$P < 0.03$). (*H*) Diagram illustrating that Lhx2 overexpression appears to interfere with and suppress NICD-induced astrogliogenesis. (Scale bars: 20 μm.) *A, B, D*, and *E* are composites assembled from multiple confocal images.

The explant culture assay reliably recapitulated the in vivo results obtained by overexpressing NICD. Whereas NICD + GFP electroporation resulted in a strong phenotype, similar to that seen with ClimΔDD (Fig. 5 *F* and *K*), coelectroporation of Lhx2-GFP rescued neurogenesis and resulted in explants with axons that resembled the controls (Fig. 5 *E* and *K*). Next, we used embryos from *Nfia*$^{+/-}$ matings, which gave us both *Nfia* mutant embryos as well as littermate controls. The control embryos, as expected, always gave explants with axons when electroporated with GFP (100%, Fig. 5 *G* and *K*). When electroporated with ClimΔDD, only 11% of the explants had detectable axons (Fig. 5 *H* and K). *Nfia* mutant explants, when electroporated with GFP, all gave explants with axons (100%), which is expected because Nfia is not known to be required for neurogenesis (Fig. 5 *I* and *K*). Strikingly, when *Nfia* mutant explants were electroporated with ClimΔDD, we observed axons in 100% of the explants (Fig. 5 *J* and *K*). This shows that ClimΔDD cannot produce astrocytes unless Nfia is functional and reveals an interaction between Lhx2 and Nfia in regulating astrogliogenesis.

This finding is also supported by experiments in which we used the γ-secretase inhibitor *N*-[*N*-(3,5-difluorophenacetyl)-l-alanyl]-*S*-phenylglycine t-butyl ester (DAPT) in experiments involving NICD or ClimΔDD (Fig. S4). Electroporated explants were incubated in 1 μM DAPT on only the first day of the 6-d culture period, after which the DAPT medium was washed out and replaced with normal medium. This limited dose and duration were sufficient to prevent activation and cleavage of the membrane-bound NICD construct, resulting in explants with robust axonal growth (Fig. S4) that resembled control GFP electroporated cultures exposed to the same DAPT treatment. Like the NICD explants, ClimΔDD electroporated explants treated with DAPT also appeared unable to induce astrogliogenesis, and instead produced axonal growth (Fig. S4).

Together, these experiments indicate that astrogliogenesis produced by ClimΔDD electroporation is dependent on an active Notch-Nfia pathway and cannot not occur in *Nfia* mutant explants or explants treated with the Notch inhibitor DAPT. The role of Lhx2 therefore appears to be to interact with and inhibit this signaling pathway during the neurogenic period.

Lhx2 Can Suppress Nfia-Induced Astrogliogenesis. We further tested the Lhx2-Nfia interaction by electroporating vectors expressing full-length Nfia alone or together with full-length Lhx2. In the control GFP electroporation, 35% of the GFP cells were astrocytes (Fig. 3 *A*, *B*, and *I*). When Nfia-GFP is overexpressed, 63% of the electroporated cells were astrocytes (Fig. 6 *A* and *I*). Coelectroporation of Lhx2-red fluorescent protein (RFP) together with Nfia-GFP is able to rescue neurogenesis, such that only 13% of the electroporated cells were astrocytes (Fig. 6 *B* and *I*). Significantly, the cells expressing Lhx2-RFP are seen to take positions within the pyramidal cell layer and display neuronal morphologies, even though they express Nfia-GFP (Fig. 6 *C* and *H*).

Because Lhx2 appears to be able to suppress Nfia-induced astrogliogenesis robustly, we tested whether Lhx2 regulates GFAP, one of the major targets of Nfia (26). We used a 2.1 kb fragment of the GFAP promoter that has been previously reported in studies involving Nfia (27). This region of the GFAP promoter has three Nfia binding sites (11). A luciferase assay using this promoter showed that Nfia activates the promoter above the baseline level. Lhx2 is able to suppress baseline activation as well as Nfia-induced activation of the GFAP promoter (Fig. 6*J*). This reveals a previously undescribed role for Lhx2 as a transcriptional repressor.

The role of Lhx2 therefore appears to be that of a brake on astrogliogenic pathways in the hippocampus during the neurogenic phase of development so as to ensure the production of sufficient numbers of neurons. If this is the case, how are astrocytes produced at all? The finding that ClimΔDD electroporated cells do not become astrocytes in *Nfia*$^{-/-}$ explants indicates that Lhx2 and Nfia are likely to act in the same cells to regulate this cell fate decision. We examined *Lhx2*, *Notch1*, and *Nfia* expression at a range of developmental stages, from predominantly neurogenic (E12) to predominantly gliogenic [postnatal day (P) 0]. *Notch1* is intensely expressed in hippocampal ventricular zone progenitors at E12 and E15. *Nfia* mRNA expression seems to be relatively weak in the hippocampal ventricular zone at all stages examined (Fig. S5), but the protein is known to be robustly expressed in hippopcampal progenitors from E14 to E18 (11). In contrast, *Lhx2* expression displays a dynamic regulation. It is intensely expressed in the hippo-

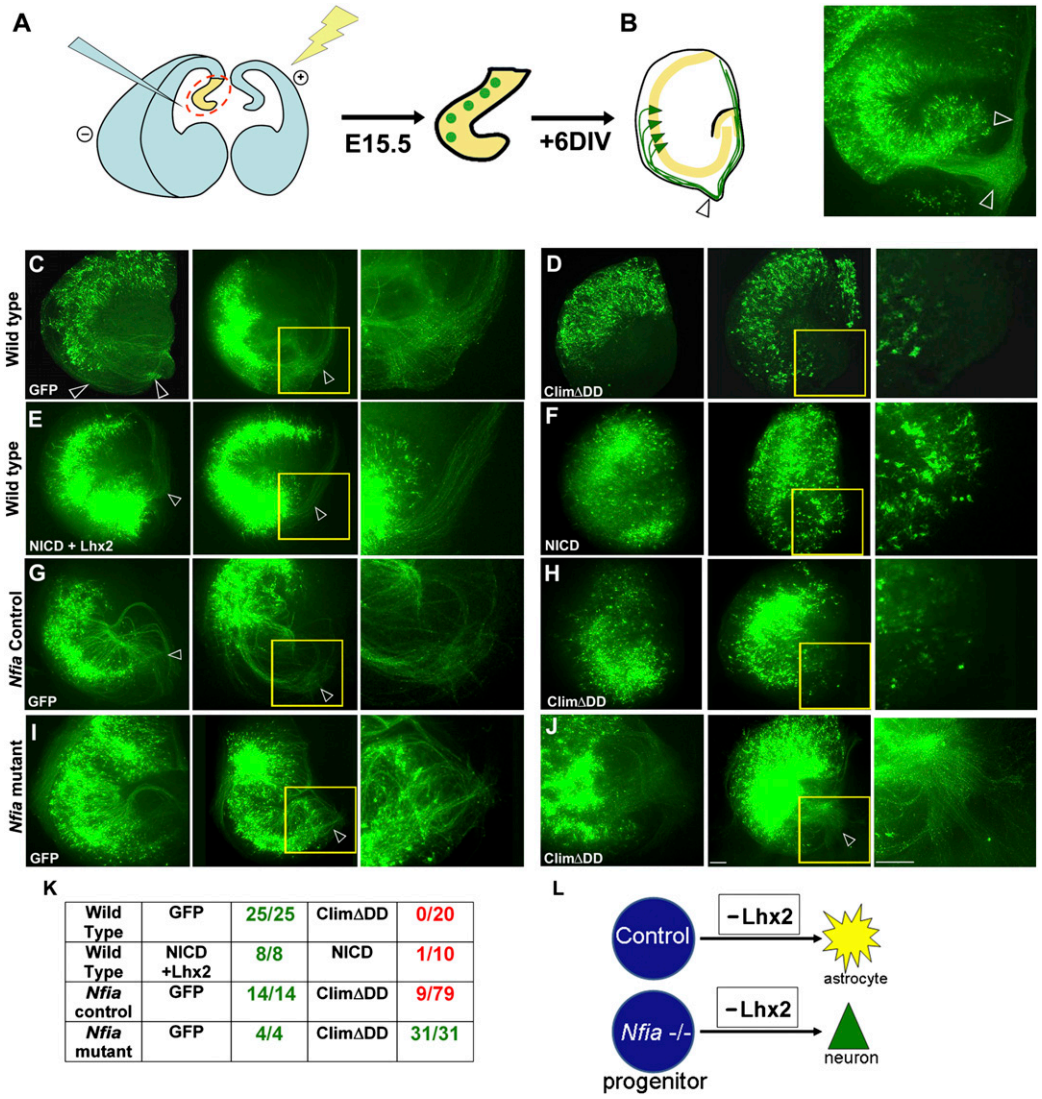

Wild Type	GFP	25/25	ClimΔDD	0/20
Wild Type	NICD +Lhx2	8/8	NICD	1/10
Nfia control	GFP	14/14	ClimΔDD	9/79
Nfia mutant	GFP	4/4	ClimΔDD	31/31

Fig. 5. In vitro organotypic explant culture system recapitulates the in utero electroporation findings and reveals interaction between Nfia and ClimΔDD in hippocampal astrogliogenesis. (*A*) Schematic of ex vivo electroporation and explant culture. After electroporation is performed in the intact brain, sections are prepared that contain electroporated progenitors (green circles). (*B*) After 6 d in vitro, the explants display GFP-expressing pyramidal neurons (green triangles) residing within the pyramidal cell layer (yellow) and extending axons (green) that encircle the periphery of the explant. A control explant electroporated with GFP is displayed alongside the schematic. Open arrowheads mark the fimbria and encircling axons. DIV, days in vitro. (*C*) Organotypic explant cultures prepared at E15, electroporated with a control (GFP) construct and examined 6 d later (+6 DIV) display robust axon bundles. Electroporation of either ClimΔDD (*D*) or NICD (*F*) switches the electroporated cells to an astrocytic fate, and axon bundles are no longer detectable. (*E*) Coelectroporation of Lhx2-GFP together with NICD rescues neurogenesis and produces a phenotype indistinguishable from control GFP electroporations (compare *C* and *E*). (*G–J*) E15 littermate embryos from $Nfia^{+/-}$ matings were used. Control (*G*) and mutant (*I*) explants electroporated with a GFP construct display numerous axons after 6 DIV, indicating proper differentiation of the pyramidal cells in the presence as well as absence of Nfia. (*H*) Electroporation of ClimΔDD-GFP in control explants produces GFP-expressing cells that do not produce axons in most of the explants. This is consistent with the astrogliogenic effect of ClimΔDD in WT brains shown in *D*. (*J*) In contrast, ClimΔDD-GFP electroporation into $Nfia^{-/-}$ explants produces explants with robust axonal growth, indicating that ClimΔDD is not able to induce astrogliogenesis in the absence of functional Nfia. (*K*) Tabulated results of the experiments shown in *C–J*. The number of explants with detectable axons was scored. (*L*) Diagram summarizing the results. In *C–J*, the region of the fimbria (yellow box) in one of the two explants is shown at higher magnification alongside. (Scale bars: 100 μm.) *E* (first image) and *F* (second image) are composites assembled from two epifluoresence images.

campal primordium at E12 and E15 but appears to decline by P0 (Fig. S5). Thus, in vivo, Lhx2 levels may drop sufficiently by late embryogenesis to permit Nfia-mediated astrogliogenesis to take off. Indeed, when Lhx2 levels were increased by overexpression at E17, the normally high level of astrogliogenesis was suppressed to a level normally seen at E15 (79–31%, Fig. 3).

Lhx2 Loss of Function Does Not Cause Premature Astrogliogenesis in the Neocortex. Because *Lhx2* is expressed in the lateral telencephalic ventricular zone up to E15 (4) (Fig. S5), we examined whether it also suppresses astrogliogenesis in neocortical progenitors. Surprisingly, neither Cre electroporation in the *Lhx2* cKO embryos nor ClimΔDD electroporation in WT E15 embryos appeared to affect the production of neocortical neurons. In each case, electroporated cells migrated to appropriate positions in the superficial layers of the neocortex (Fig. 7 *A–C*). These cells displayed the expected morphology of cortical pyramidal neurons and extended axons, and they coexpressed the neuronal marker β-tubulin but did not express GFAP (Fig. 7 *B–E*). In contrast to the results in the hippocampus, no increase in

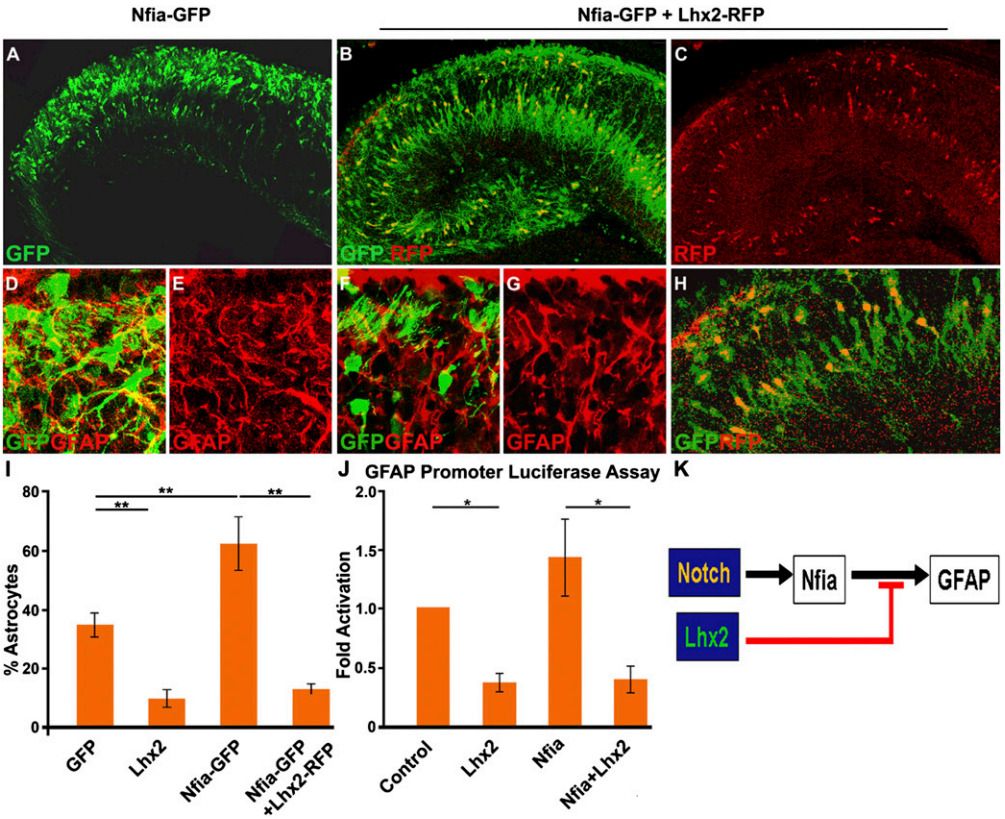

Fig. 6. Lhx2 can override Nfia-induced astrocytic cell fate specification in vivo. (*A*) In utero electroporation of full-length Nfia-GFP (green) increases the GFAP-expressing fraction from control levels (35%, Fig. 3*A*) to 63%, consistent with the known astrogliogenic effect of Nfia. (*D* and *E*) High-magnification confocal images of the GFP and GFAP channels. GFP is false-colored green, and GFAP is false-colored red. (*B*) When Lhx2-RFP (red) is coelectroporated with Nfia-GFP (green), only 13% of the GFP-expressing cells coexpress GFAP. The cells expressing Lhx2-RFP were detected by directly imaging the section for RFP fluorescence. (*F* and *G*) High-magnification confocal images of the GFP (false-colored green) and GFAP (false-colored red) channels. (*C*) Confocal image of the RFP expression (indicating Lhx2-RFP expression) of the section in *B* reveals that the RFP cells preferentially localize to the pyramidal cell layer. (*H*) High-magnification confocal image overlay of the GFP-RFP channels with yellow coexpressing cells. (*I*) GFP-expressing cells were scored. In control (GFP electroporated) brains, 35% of the GFP-expressing cells were also GFAP-positive (Fig. 3). This number decreased to 10% with Lhx2 overexpression (Fig. 3) and increased to 63% in brains overexpressing Nfia-GFP. In Nfia-GFP + Lhx2-RFP coelectroporated brains, astrogliogenesis decreased to 13%. The bars represent the mean ± SD (**$P < 0.001$). (*J*) Length of 2,100 bp of the murine GFAP promoter was used in a luciferase reporter assay in U87mg cells. Compared with cells transfected with the GFAP-luciferase vector alone, cotransfection with Lhx2 resulted in 0.4-fold (±0.08) repression, whereas contransfection with Nfia alone resulted in 1.5-fold (±0.32) activation of the reporter. Cotransfection with both Nfia and Lhx2 resulted in 0.4-fold (±0.11) repression, indicating that Lhx2 is able to override and suppress Nfia-induced activation of the GFAP promoter. The bars represent the mean ± SD (*$P < 0.08$). (*K*) Diagram of the molecular mechanism of the Lhx2-Notch pathway interaction. Notch activation induces a gliogenic target, Nfia, which, in turn, activates the GFAP promoter. Lhx2 overrides Nfia-induced GFAP activation. (Scale bars: *A–C*, 100 μm; *D–H*, 20 μm.) *A–H* are composites assembled from multiple confocal images.

astrogliogenesis was seen in the neocortex of ClimΔDD electroporated brains (Fig. 7*F*). We also examined this question at an earlier stage, E13, when deep-layer neurons are normally produced. Four days after electroporation, ClimΔDD cells had migrated to the cortical plate and extended apical dendrites as well as axons that coursed through the intermediate zone, similar to control GFP electroporated cells (Fig. S6). Therefore, Lhx2 does not suppress astrogliogenesis in the neocortex, revealing a surprising spatial restriction for this role.

Discussion

Our study reveals a critical role for Lhx2 in regulating neuronal vs. astrocytic cell fate in the hippocampus. This is a previously undescribed role for the LIM-HD family and extends the established role for members of this group in regulating cell fate across several systems. Apterous, the *Drosophila* ortholog of Lhx2, functions as a dorsal selector gene in the wing and also regulates neurotransmitter identity in the ventral nerve cord (28, 29). Similarly, other members of the LIM-HD family determine motor neuron vs. interneuron fate in the vertebrate spinal cord and also instruct particular motor neuron subtype identities (30). Our study reports LIM-HD gene function in the fundamental step of regulating neuronal vs. nonneuronal cell fate.

Lhx2 Is Necessary and Sufficient for Suppressing Hippocampal Astrogliogenesis. In the hippocampus, E12 to E16 is the predominantly neurogenic phase, after which gliogenesis peaks. However, gliogenic pathways in this system have not been well studied. Notch and Nfia, two well-studied instructive molecules for neocortical gliogenesis, are expressed in hippocampal progenitors right from the beginning of the neurogenic phase (31) (Fig. S5). Lhx2 plays a critical role in hippocampal progenitors by interacting with these known progliogenic regulators, serving as a necessary and sufficient cell intrinsic repressor of gliogenesis.

Lhx2-Notch Pathway Interaction Regulates the Timing of the Neuron-Glia Cell Fate Switch. In the *Drosophila* wing, Apterous extensively interacts with the Notch pathway (32). Our results reveal an elegant functional interaction between these two cell fate regulators, such that cell fate in the developing hippocampus appears to depend on the balance between these two pathways. Our data indicate that Lhx2 acts as a brake on astrogliogenesis. Endoge-

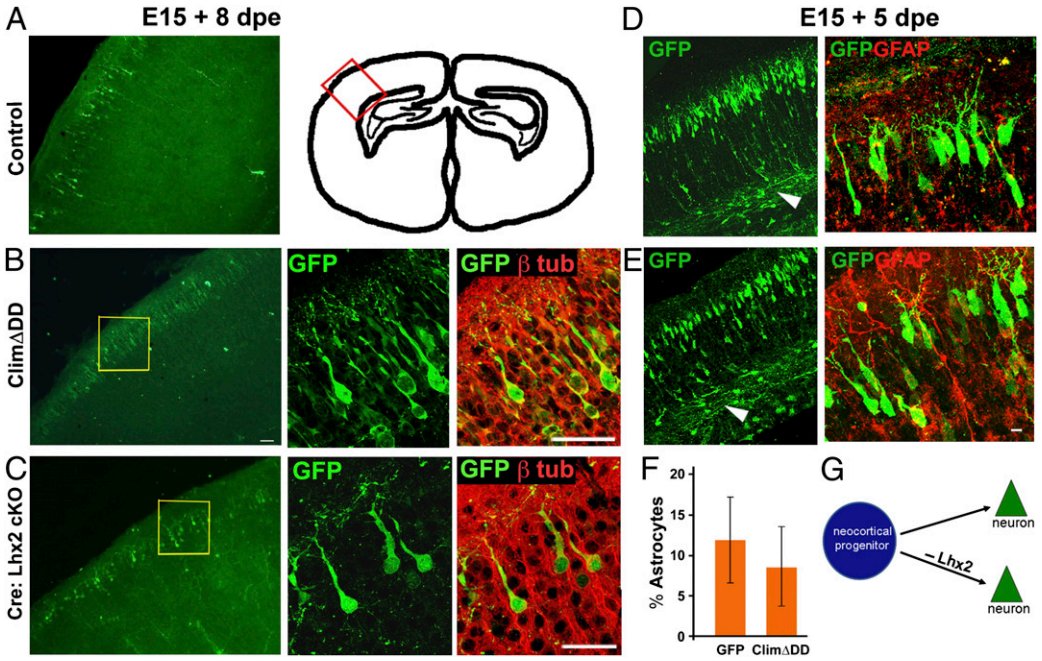

Fig. 7. Loss of Lhx2 function does not cause premature astrogliogenesis in the neocortex. (*A* and *D*) Control *GFP* construct electroporated into WT embryos at E15 labels cells that migrate to the superficial layers of the neocortex. These cells display characteristic pyramidal neuronal morphologies and send axonal projections via the white matter (*D*, arrowhead). The schematic in *A* illustrates the region of the neocortex from which the cells were imaged. Similar results are seen when ClimΔDD is electroporated into a WT embryo (*B* and *E*) or when a *Cre-GFP* construct is electroporated into *Lhx2* cKO embryos (*C*). dpe, days postelectroporation. Confocal images of the boxed regions in *B* and *C* show that the electroporated cells have characteristic pyramidal neuronal morphologies and express the neuronal marker β(III) tubulin. (*D* and E) Both control and ClimΔDD electroporated cells produce cells that extend axons into the white matter and do not coexpress GFAP. (*F*) GFP- and GFAP-expressing cells were scored in electroporated brains. Similar proportions of cells coexpressed these proteins in control (12%) and ClimΔDD (8.6%) brains (not significant; $P > 0.05$). (*G*) Diagram illustrates that loss of Lhx2 function in neocortical progenitors does not appear to affect neurogenesis. (Scale bars: 20 μm.) *D* and *E* are composites assembled from multiple images.

nous *Lhx2* expression in hippocampal progenitors is intense during the neurogenic phase and declines when gliogenesis peaks. Down-regulation of Lhx2 in the progenitors in the neurogenic phase causes premature astrogliogenesis. Either constitutive Notch activation or Nfia overexpression during the neurogenic phase also tips the balance toward astrogliogenesis, but simultaneous overexpression of Lhx2 is able to rescue neurogenesis. Overexpression of Lhx2 in the gliogenic phase prolongs neurogenesis. This suggests a model in which high levels of Lhx2 act to repress Notch/Nfia-mediated astrogliogenesis until neurogenesis is complete. A decline in Lhx2 levels may then release the brake on astrogliogenesis, which then becomes the predominant differentiation program from late embryonic stages onward. Thus, Lhx2 level in the progenitor may control the correct timing of the neuron-glia cell fate switch.

Notch activation promotes astrogliogenesis via Nfia (9–11) and also via other target genes, such as Hes1, Hes5, Hesr1, and Hesr2 (33–35). Notch signaling also interacts with the JAK-STAT pathway to promote astrogliogenesis (7, 36). This may explain why coelectroporation of Lhx2 suppresses Notch-induced astrogliogenesis only partially (69% decreasing to 51%) but appears to achieve a dramatic suppression of Nfia-induced astrogliogenesis (63% decreasing to 13%). This indicates a highly specific point of interaction of Lhx2 with the Notch pathway in suppressing the astrogliogenic effects of the Notch target Nfia. Removing Lhx2 does not produce astrocytes unless Nfia is functional. This indicates that astrocytes produced as a result of loss of Lhx2 are generated by the Notch-Nfia pathway rather than an independent pathway. Lhx2 therefore interacts with this pathway to suppress its astrogliogenic function.

Lhx2 Has Temporally Distinct Roles. Before E10.5 in the dorsal telencephalon, Lhx2 acts as a cortical selector, where it is required for specifying cortical (hippocampus + neocortex) identity and repressing noncortical (hem/antihem) fates (3). At later stages, in hippocampal progenitors, Lhx2 controls the fundamental neuron-astrocyte cell fate decision, such that it promotes neurogenesis by suppressing astrogliogenesis.

Notch signaling is also known to have multiple roles in the telencephalic neuroepithelium, an early role in maintaining proliferation of the progenitor pool (37), and a later role in instructing astrogliogenesis (22, 7).

Interestingly, Notch and Lhx2 appear to have parallel early roles in maintaining the proliferation and cortical identity of neuroepithelial progenitors, respectively. In contrast, they play opposing roles in regulating the cell fate of the postmitotic progeny arising from these progenitors, such that Notch is progliogenic and Lhx2 suppresses gliogenesis. How the balance between these opposing players is controlled to generate the choreography of neurogenesis followed by astrogliogenesis remains a compelling open question.

Context-Specific Control of Cell Fate. Well-characterized cell fate specification regulators, such as the PDGF, BDNF, Notch, and JAK-STAT pathways or the cell fate determining transcription factor Ngn2, have not been reported to have spatially regulated actions in the developing telencephalon. What mechanisms might underlie the striking disparity in Lhx2 dependence we observe between hippocampal and neocortical progenitors? One unique feature of the medial telencephalon is that it experiences high levels of Wnt signaling, which is an important determinant of neuronal fate in progenitors (38). Several Wnt genes and their receptors are expressed in the medial telencephalic wall (39, 40).

Lef1, the downstream effector of canonical Wnt signaling, is also expressed at high levels medially and tapers off laterally (41). A strong medial source of multiple Wnt family members, the cortical hem (39), is itself regulated by Lhx2, which limits the extent of the hem by repressing hem fate (3). The combination of high levels of Wnt signaling and high levels of Lhx2 in the medial telencephalon may initiate a program of cell fate regulation whose effect is unique to this region. Thus, Lhx2 itself might be a key participant in the fundamental mechanism that determines the regional specificity of cell fate control mechanisms. Diversity within the broad category of astrocytes is beginning to be appreciated (42), and it is possible that the regional disparity we report in the regulation of astrocyte production also confers a unique identity to hippocampal astrocytes.

Materials and Methods

DNA Constructs. EGFP, Cre-GFP, Lhx2-GFP, Lhx2-RFP, Nfia-GFP, NICD expression plasmids, and the GFAP promoter-luciferase plasmid are detailed in *SI Materials and Methods*.

In Utero Electroporation. All procedures followed the Institutional Animal Ethics Committee guidelines. The *Lhx2* cKO mice used in this study have been described previously (3).

Immunostaining. The sources, concentrations, and protocols for the antibodies used in this study [rabbit anti-GFP, biotinylated goat anti-GFP, chicken anti-GFP, rabbit anti-GFAP, mouse monoclonal anti-β(III) tubulin isoform, goat anti-Aldo C, rabbit anti-Ki67, rabbit anti-ACTIVE caspase-3, and rabbit anti-Olig2] are detailed in *SI Materials and Methods*.

Imaging. The different epifluorescence, Apotome (Zeiss), and confocal microscopes used are described in *SI Materials and Methods*, together with image analysis procedures used.

In Situ Hybridization. In situ hybridization was performed as described by Bulchand et al. (4).

GFAP Promoter Luciferase Assay. U87mg cells (kind gift from Neelam Shirsat, The Advanced Centre for Treatment, Research and Education in Cancer, Navi Mumbai 410210, India) were used in a standard luciferase assay. The detailed protocol is described in *SI Materials and Methods*.

Statistical Analysis. Statistical analysis was done using the unpaired *t* test and GraphPad In-Stat and SigmaPlot Software. The results are expressed as the mean ± SD. For each control and experimental condition, 100 or more cells were counted from sections taken from three to four different electroporated embryos.

Ex Utero Electroporation and Explant Culture. This protocol is described in *SI Materials and Methods*.

ACKNOWLEDGMENTS. We thank L. Carlsson, F. Guillemot, T. Ohshima, T. Saito, G. Weinmaster, L. Mucke, and J. J. He for kind gifts of DNA constructs; Y. Nakagawa and F. Porter for plasmids used for generating probes; and N. Shirsat for the U87 cell line. We thank V. Suryavanshi, S. Kothawale, and K. Kadam for assistance with the in utero surgical procedures over the duration of this project; V. Kinare for assistance with figure preparation; and B. Tursun for Fig. S1*A*. We thank S. K. McConnell and members of the McConnell laboratory for input and discussions during the sabbatical year of S.T. We appreciate the excellent support of Dr. S. Suryavanshi and the Tata Institute of Fundamental Research Animal House staff. This work was supported by a Wellcome Trust Senior Fellowship (056684/Z/99/Z), a Swarnajayanti Fellowship (4/3/2005-SF), and grants from the Department of Science and Technology, Government of India (SR/SO/BB-44/2004) and the Department of Biotechnology, Government of India (to S.T.), as well as by a Kanwal Rekhi Career Development Award from the Tata Institute of Fundamental Research Endowment Fund (to L.S. and H.P.). M.P. and L.J.R. are supported by a Career Development Award and a Principal Research Fellowship, respectively, from the National Health and Medical Research Council, Australia.

1. Bulchand S, Grove EA, Porter FD, Tole S (2001) LIM-homeodomain gene Lhx2 regulates the formation of the cortical hem. *Mech Dev* 100:165–175.
2. Monuki ES, Porter FD, Walsh CA (2001) Patterning of the dorsal telencephalon and cerebral cortex by a roof plate-Lhx2 pathway. *Neuron* 32:591–604.
3. Mangale VS, et al. (2008) Lhx2 selector activity specifies cortical identity and suppresses hippocampal organizer fate. *Science* 319:304–309.
4. Bulchand S, Subramanian L, Tole S (2003) Dynamic spatiotemporal expression of LIM genes and cofactors in the embryonic and postnatal cerebral cortex. *Dev Dyn* 226: 460–469.
5. Miller FD, Gauthier AS (2007) Timing is everything: Making neurons versus glia in the developing cortex. *Neuron* 54:357–369.
6. Mizutani K, Saito T (2005) Progenitors resume generating neurons after temporary inhibition of neurogenesis by Notch activation in the mammalian cerebral cortex. *Development* 132:1295–1304.
7. Ge W, et al. (2002) Notch signaling promotes astrogliogenesis via direct CSL-mediated glial gene activation. *J Neurosci Res* 69:848–860.
8. Shu T, Butz KG, Plachez C, Gronostajski RM, Richards LJ (2003) Abnormal development of forebrain midline glia and commissural projections in Nfia knock-out mice. *J Neurosci* 23:203–212.
9. Deneen B, et al. (2006) The transcription factor NFIA controls the onset of gliogenesis in the developing spinal cord. *Neuron* 52:953–968.
10. Namihira M, et al. (2009) Committed neuronal precursors confer astrocytic potential on residual neural precursor cells. *Dev Cell* 16:245–255.
11. Piper M, et al. (2010) NFIA controls telencephalic progenitor cell differentiation through repression of the Notch effector Hes1. *J Neurosci* 30:9127–9139.
12. Altman J, Bayer SA (1990) Prolonged sojourn of developing pyramidal cells in the intermediate zone of the hippocampus and their settling in the stratum pyramidale. *J Comp Neurol* 301:343–364.
13. Rickmann M, Amaral DG, Cowan WM (1987) Organization of radial glial cells during the development of the rat dentate gyrus. *J Comp Neurol* 264:449–479.
14. Matthews JM, Visvader JE (2003) LIM-domain-binding protein 1: A multifunctional cofactor that interacts with diverse proteins. *EMBO Rep* 4:1132–1137.
15. Bach I, et al. (1999) RLIM inhibits functional activity of LIM homeodomain transcription factors via recruitment of the histone deacetylase complex. *Nat Genet* 22: 394–399.
16. Becker T, et al. (2002) Multiple functions of LIM domain-binding CLIM/NLI/Ldb cofactors during zebrafish development. *Mech Dev* 117:75–85.
17. Zhao Y, et al. (1999) Control of hippocampal morphogenesis and neuronal differentiation by the LIM homeobox gene Lhx5. *Science* 284:1155–1158.
18. Walther EU, et al. (1998) Genomic sequences of aldolase C (Zebrin II) direct lacZ expression exclusively in non-neuronal cells of transgenic mice. *Proc Natl Acad Sci USA* 95:2615–2620.
19. Cahoy JD, et al. (2008) A transcriptome database for astrocytes, neurons, and oligodendrocytes: A new resource for understanding brain development and function. *J Neurosci* 28:264–278.
20. Dugas JC, et al. (2010) Dicer1 and miR-219 are required for normal oligodendrocyte differentiation and myelination. *Neuron* 65:597–611.
21. Ligon KL, Fancy SP, Franklin RJ, Rowitch DH (2006) Olig gene function in CNS development and disease. *Glia* 54:1–10.
22. Chambers CB, et al. (2001) Spatiotemporal selectivity of response to Notch1 signals in mammalian forebrain precursors. *Development* 128:689–702.
23. Oakley F, et al. (2003) Basal expression of IkappaBalpha is controlled by the mammalian transcriptional repressor RBP-J (CBF1) and its activator Notch1. *J Biol Chem* 278:24359–24370.
24. Tole S, Christian C, Grove EA (1997) Early specification and autonomous development of cortical fields in the mouse hippocampus. *Development* 124:4959–4970.
25. Becker N, Wierenga CJ, Fonseca R, Bonhoeffer T, Nägerl UV (2008) LTD induction causes morphological changes of presynaptic boutons and reduces their contacts with spines. *Neuron* 60:590–597.
26. Cebolla B, Vallejo M (2006) Nuclear factor-I regulates glial fibrillary acidic protein gene expression in astrocytes differentiated from cortical precursor cells. *J Neurochem* 97:1057–1070.
27. Zhou BY, Liu Y, Kim B, Xiao Y, He JJ (2004) Astrocyte activation and dysfunction and neuron death by HIV-1 Tat expression in astrocytes. *Mol Cell Neurosci* 27:296–305.
28. Blair SS, Brower DL, Thomas JB, Zavortink M (1994) The role of apterous in the control of dorsoventral compartmentalization and PS integrin gene expression in the developing wing of Drosophila. *Development* 120:1805–1815.
29. Benveniste RJ, Thor S, Thomas JB, Taghert PH (1998) Cell type-specific regulation of the Drosophila FMRF-NH2 neuropeptide gene by Apterous, a LIM homeodomain transcription factor. *Development* 125:4757–4765.
30. Shirasaki R, Pfaff SL (2002) Transcriptional codes and the control of neuronal identity. *Annu Rev Neurosci* 25:251–281.
31. Plachez C, et al. (2008) Nuclear factor I gene expression in the developing forebrain. *J Comp Neurol* 508:385–401.
32. Milán M, Cohen SM (2000) Temporal regulation of apterous activity during development of the Drosophila wing. *Development* 127:3069–3078.
33. Hojo M, et al. (2000) Glial cell fate specification modulated by the bHLH gene Hes5 in mouse retina. *Development* 127:2515–2522.
34. Furukawa T, Mukherjee S, Bao ZZ, Morrow EM, Cepko CL (2000) rax, Hes1, and notch1 promote the formation of Müller glia by postnatal retinal progenitor cells. *Neuron* 26:383–394.

35. Sakamoto M, Hirata H, Ohtsuka T, Bessho Y, Kageyama R (2003) The basic helix-loop-helix genes Hesr1/Hey1 and Hesr2/Hey2 regulate maintenance of neural precursor cells in the brain. *J Biol Chem* 278:44808–44815.
36. Kamakura S, et al. (2004) Hes binding to STAT3 mediates crosstalk between Notch and JAK-STAT signalling. *Nat Cell Biol* 6:547–554.
37. Louvi A, Artavanis-Tsakonas S (2006) Notch signalling in vertebrate neural development. *Nat Rev Neurosci* 7:93–102.
38. Hirabayashi Y, et al. (2004) The Wnt/beta-catenin pathway directs neuronal differentiation of cortical neural precursor cells. *Development* 131:2791–2801.
39. Grove EA, Tole S, Limon J, Yip L, Ragsdale CW (1998) The hem of the embryonic cerebral cortex is defined by the expression of multiple Wnt genes and is compromised in Gli3-deficient mice. *Development* 125:2315–2325.
40. Kim AS, Anderson SA, Rubenstein JL, Lowenstein DH, Pleasure SJ (2001) Pax-6 regulates expression of SFRP-2 and Wnt-7b in the developing CNS. *J Neurosci* 21:RC132.
41. Galceran J, Miyashita-Lin EM, Devaney E, Rubenstein JL, Grosschedl R (2000) Hippocampus development and generation of dentate gyrus granule cells is regulated by LEF1. *Development* 127:469–482.
42. Freeman MR (2010) Specification and morphogenesis of astrocytes. *Science* 330:774–778.

Supporting Information

Subramanian et al. 10.1073/pnas.1101109108

SI Materials and Methods

DNA Constructs. ***Cre-GFP.*** A construct encoding Cre recombinase together with an EGFP reporter cassette, pCIG (*Cre-IRES-EGFP*), was gifted to us by F. Guillemot (Medical Research Council National Institute for Medical Research, London, UK).
Lhx2-GFP and Lhx2-RFP. Dual-promoter vectors, *pCGC* and pCRC, which express EGFP and RFP, respectively, downstream of the first *CAG* promoter were used (gift from Toshio Ohshima, Waseda University, Tokyo, Japan). A 1.2-kb EcoRI digest of *pcDNA3.1-Lhx2* (gift from Leif Carlsson, Umeå Centre for Molecular Medicine, Umeå, Sweden) containing the *Lhx2* ORF was ligated into the EcoR1 site downstream of the second *CAG* promoter.
pCAG-ClimΔDD-IRES2-EGFP. The 551-bp BamHI digest product (corresponding to amino acids 225–341 of the Clim1a protein) from *pCS2-ClimΔDD* (1) was ligated into the BamHI site of *pCAG-IRES2-EGFP*.
Nfia-GFP. A 1,530-bp EcoRI digest product containing *Nfia* sequence from pCMV-*Nfia* (2) was ligated into the EcoRI site of pCAGIG.
GFAP promoter plasmid. A GFAP-luciferase plasmid was obtained from J. J. He (Indiana University School of Medicine, Indianapolis, IN) with the kind permission of L. Mucke (The Scripps Research Institute, La Jolla, CA) (3). This plasmid contains the 2.1-kb region upstream of the transcription start site of the murine GFAP gene, followed by the luciferase ORF.
EGFP. The *pCAG-IRES2-EGFP* was a gift from T. Saito (Institute for Frontier Medical Sciences, Kyoto University, Kyoto, Japan).
NICD. *pEF-ZEDN1*, which encodes constitutively active Notch1 (4, 5), was a gift from Gerry Weinmaster (University of California, Los Angeles, CA). Because this construct did not have a GFP reporter, we mixed it before electroporation with the EGFP construct (2:1 NICD/EGFP). This ratio increases the likelihood that all EGFP-expressing cells also expressed NICD. This practice of mixing plasmids for coelectroporation is well established in the literature and produces reliable coexpression in 99% of the cells (6–8).

In Utero Electroporation. All procedures followed the Institutional Animal Ethics Committee guidelines. The *Lhx2* cKO mice used in this study have been described previously by Mangale et al. (9). Male mice used were heterozygous for a standard *Lhx2* null allele [standard knockout (sKO)] (10) and were also heterozygous for a floxed *Lhx2* allele (cKO) (9). The female mice were heterozygous for only the *Lhx2* cKO allele. Such matings generate sKO/cKO and cKO/cKO embryos, into which Cre electroporation results in recombination of the floxed alleles and produces an *Lhx2* null cell. Littermate controls are +/sKO embryos, which are unaffected by Cre recombinase. The *Nfia* KO mice used were described previously (11). Embryos were genotyped by PCR (12).

For electroporation into WT mice, Swiss mice were obtained from the Tata Institute of Fundamental Research animal breeding facility. A total of 2.5% (wt/vol) avertin [1-g/mL solution of 2, 2, 2-Tribromoethanol, 97% in tert-amylalcohol (99+%); Aldrich, catalog nos. T4,840-2 and 24,048-6, respectively] in 0.9% saline was injected i.p. (15 μL/g of body weight) to anesthetize E15.5-timed pregnant mice. Electroporation was carried out as described by Saito and Nakatsuji (13). A 1-cm laparotomy was performed, and the uterus with the embryos was exposed. A total of 4–5 μL of plasmid DNA [approximately 1 μg/μL, dissolved in Tris (10 mM) EDTA (0.1 mM) buffer, pH 8.0] prepared using the Qiagen Plasmid Maxi Kit (catalog no. 12163) was injected into the lateral ventricle using a fine-glass microcapillary. Electroporation was performed using a BTX Electro Square Porator ECM 830 or a Nepagene CUY21 electroporator [40 V (E15.5), 5 pulses, 50-ms pulse length, ∼1.0-s pulse interval]. For delivering electrical pulses, paddle electrodes (7-mm diameter) were used with the positive side directed to the medial wall of the ventricle into which the DNA was injected. Uterine horns were repositioned into the abdominal cavity, and the abdominal wall and skin were sewed with surgical sutures. Mice were kept on a warm plate (37 °C) for recovery. Six to eight days after electroporation, pups were anesthetized on ice and transcardially perfused with 4% (wt/vol) paraformaldehyde (PFA; Sigma) made in 0.1 M phosphate buffer (pH 7.4). After 24 h in 4% (wt/vol) PFA, the brains were transferred to 30% (wt/vol) sucrose solution in 4% (wt/vol) PFA. They were sectioned at 30 μm using a freezing microtome (Leica). Serial sections were analyzed by immunohistochemistry and in situ hybridization.

Immunostaining. The following primary antibodies were used: rabbit anti-GFP (1:250/500; Molecular Probes, catalog no. A11122), biotinylated goat anti-GFP (1:500; Abcam, catalog no. ab6658), chicken anti-GFP (1:500; Aves Labs, catalog no. GFP-1020), mouse monoclonal anti-β(III) tubulin isoform (1:250; Chemicon, catalog no. MAB1637), rabbit anti-GFAP (1:250; Sigma, catalog no. G9269), goat anti-AldoC (1:50; Santa Cruz Biotech, catalog no. sc12066), rabbit anti-Ki67 (1:200; Abcam, catalog no. ab15580), rabbit anti-ACTIVE caspase-3 (1:100; Promega, catalog no. G748A), and rabbit anti-Olig2 (1:500; Millipore, catalog no. AB9610). Secondary antibodies used were biotinylated goat anti-mouse (1:250; Molecular Probes, catalog no. B2763) or biotinylated goat anti-rabbit (1:100; Chemicon, catalog no. AP156B). The fluorophores were Streptavidin Alexa 568 (1:250; Molecular Probes, catalog no. S11226) and Alexa 680 (1:250, Molecular Probes, catalog no. S32358) for β(III) tubulin and GFAP and goat anti-rabbit or goat anti-chicken antibody conjugated to Alexa 488 (1:250; Molecular Probes, catalog nos. A11008 and A11039) for GFP. Streptavidin Alexa 488 (1:250; Molecular Probes, catalog no. S11223) was used directly at a ratio of 1:250 when biotinylated goat anti-GFP was used.

The brains were sectioned (30 μm) using a freezing microtome. The sections were mounted on Superfrost Plus slides (Erie Scientific Company) and fixed in 4% (wt/vol) PFA for 5 min at room temperature (RT) and washed with 0.1 M phosphate buffer (pH 7.4). All antibodies required antigen retrieval by boiling in 10 mM sodium citrate buffer (pH 6.0) for 6 min. The slides were allowed to cool to RT and then washed with 0.1 M phosphate buffer, before blocking. Sections were blocked in 10% (vol/vol) lamb serum (Invitrogen) in 0.1 M phosphate buffer with 0.3% (vol/vol) Triton X-100 (Sigma) for 1 h at RT. This was followed by primary antibody treatment in 0.1 M phosphate buffer containing 0.3% (vol/vol) Triton X-100 and 2% (vol/vol) lamb serum overnight at RT. The sections were then washed in 0.1 M phosphate buffer, followed by biotin-labeled secondary antibody for 2 h (1:250–1:400). The slides were again washed with 0.1 M phosphate buffer and incubated with streptavidin-conjugated antibodies (1:250) for 1 h.

Imaging. Images were taken using a Zeiss Axioplan 2 plus microscope, Zeiss AxioCam camera, and Zeiss Axiovision software for epifluorescence images. For marker colocalization, individual cells in the sections were imaged at a magnification of 63× using the Zeiss Apotome scanning system (Fig. 2 *A* and *C*), Leica SP5

upright confocal (Fig. 2*E*) system, and Zeiss LSM 510 (Figs. 2–4, 6, and 7) and at a magnification of 60× using the Olympus Fluoview Confocal Imaging system (Figs. 1 and 4). Image stacks were generated by scanning at intervals of 0.5–1.0 μm using filters of the appropriate wavelengths. The stacks were analyzed, merged, and projected using ImageJ software from the National Institutes of Health. Figure panels were prepared using Adobe Photoshop.

GFAP Promoter Luciferase Assay. U87mg cells (kind gift from Neelam Shirsat, The Advanced Centre for Treatment, Research and Education in Cancer, Navi Mumbai 410210, India) were cultured in DMEM supplemented with 10% (vol/vol) FBS, penicillin (100 U/mL), and streptomycin (100 μg/mL). For transfections, 7×10^4 cells per well were seeded into 24-well plates. After an overnight incubation, the medium was removed and 2.1 kb of GFAP-promoter plasmid was added together with GFP (control), Nfia-GFP, Lhx2-RFP, or Nfia-GFP + Lhx2-RFP. Transfection was performed using 2 μL of Lipofectamine-LTX (Invitrogen) in 0.5 mL of medium and incubated for 16 h. Next, the medium-DNA mix was removed and substituted with fresh medium. Renilla luciferase (1 ng) was added to each transfection as a normalization control. Luciferase activity was measured using a commercial dual-luciferase assay system (Promega) 48 h after transfection. All the values are expressed as the mean ± SD of at least three independent experiments carried out in triplicate.

Ex Utero Electroporation and Explant Culture. The embryos were dissected out from the uterus, and the brains were removed and placed in sterile cold L-15 medium. Plasmid DNA (prepared using a Qiagen Maxi-prep kit) was injected into the ventricle of the brain. The brain was then electroporated on the medial side five times with a square-pulse of 50 V for 50 ms, with a 1-s gap between each pulse, using a BTX Electro Square Porator ECM 830 electroporator. Following this, the electroporated hemisphere was separated and the meninges were removed. The hemisphere was then sectioned at 250 μm using a McIllwain tissue chopper. The hippocampal slices were then cultured on a filter in DMEM containing B-27 supplement for 6 d in a 5% CO_2 atmosphere (14). The medium was changed on the third day. For the DAPT treatment, 1 μM DAPT was added to the medium for the first day. On the second day, the medium was changed three times to wash out residual DAPT and the explants were maintained in fresh medium.

In Vitro Protein–Protein Interaction. ^{35}S-labeled *ClimΔDD* (mouse) was expressed in vitro from the DN-CLIM-pCS2-MT plasmid (15). The Lhx2-LIM bacterial expression plasmid used was pGEX-Lhx2-LIM (14). GST pull-down experiments were performed as described by Bach et al. (1).

1. Bach I, et al. (1995) P-Lim, a LIM homeodomain factor, is expressed during pituitary organ and cell commitment and synergizes with Pit-1. *Proc Natl Acad Sci USA* 92: 2720–2724.
2. Chaudhry AZ, Lyons GE, Gronostajski RM (1997) Expression patterns of the four nuclear factor I genes during mouse embryogenesis indicate a potential role in development. *Dev Dyn* 208:313–325.
3. Johnson WB, et al. (1995) Indicator expression directed by regulatory sequences of the glial fibrillary acidic protein (GFAP) gene: In vivo comparison of distinct GFAP-lacZ transgenes. *Glia* 13:174–184.
4. Oakley F, et al. (2003) Basal expression of IkappaBalpha is controlled by the mammalian transcriptional repressor RBP-J (CBF1) and its activator Notch1. *J Biol Chem* 278:24359–24370.
5. Patten BA, Peyrin JM, Weinmaster G, Corfas G (2003) Sequential signaling through Notch1 and erbB receptors mediates radial glia differentiation. *J Neurosci* 23: 6132–6140.
6. Tabata H, Nakajima K (2008) Labeling embryonic mouse central nervous system cells by in utero electroporation. *Dev Growth Differ* 50:507–511.
7. Barnabé-Heider F, et al. (2008) Genetic manipulation of adult mouse neurogenic niches by in vivo electroporation. *Nat Methods* 5:189–196.
8. Friocourt G, et al. (2008) Cell-autonomous roles of ARX in cell proliferation and neuronal migration during corticogenesis. *J Neurosci* 28:5794–5805.
9. Mangale VS, et al. (2008) Lhx2 selector activity specifies cortical identity and suppresses hippocampal organizer fate. *Science* 319:304–309.
10. Porter FD, et al. (1997) Lhx2, a LIM homeobox gene, is required for eye, forebrain, and definitive erythrocyte development. *Development* 124:2935–2944.
11. Piper M, et al. (2010) NFIA controls telencephalic progenitor cell differentiation through repression of the Notch effector Hes1. *J Neurosci* 30:9127–9139.
12. Shu T, Butz KG, Plachez C, Gronostajski RM, Richards LJ (2003) Abnormal development of forebrain midline glia and commissural projections in Nfia knock-out mice. *J Neurosci* 23:203–212.
13. Saito T, Nakatsuji N (2001) Efficient gene transfer into the embryonic mouse brain using in vivo electroporation. *Dev Biol* 240:237–246.
14. Tole S, Christian C, Grove EA (1997) Early specification and autonomous development of cortical fields in the mouse hippocampus. *Development* 124:4959–4970.
15. Bach I, et al. (1999) RLIM inhibits functional activity of LIM homeodomain transcription factors via recruitment of the histone deacetylase complex. *Nat Genet* 22:394–399.

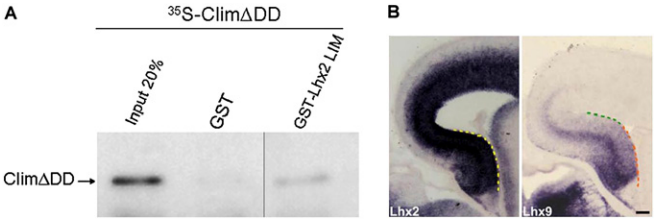

Fig. S1. (*A*) ClimΔDD binds the LIM domains of Lhx2 in a pull-down assay. (*B*) At E15, *Lhx2* is strongly expressed in the entire hippocampal ventricular zone (delineated by yellow dashed line). In contrast, *Lhx9* expression is strong in the dentate gyrus, weaker in CA3 (orange dashed lines), and tapers off in the ventricular zone of CA1 (green dashed lines). No other LIM-HD gene is expressed in the ventricular zone of the E15 hippocampus. (Scale bar: 100 μm.) One intervening lane pertaining to GST-Lhx3-LIM was removed.

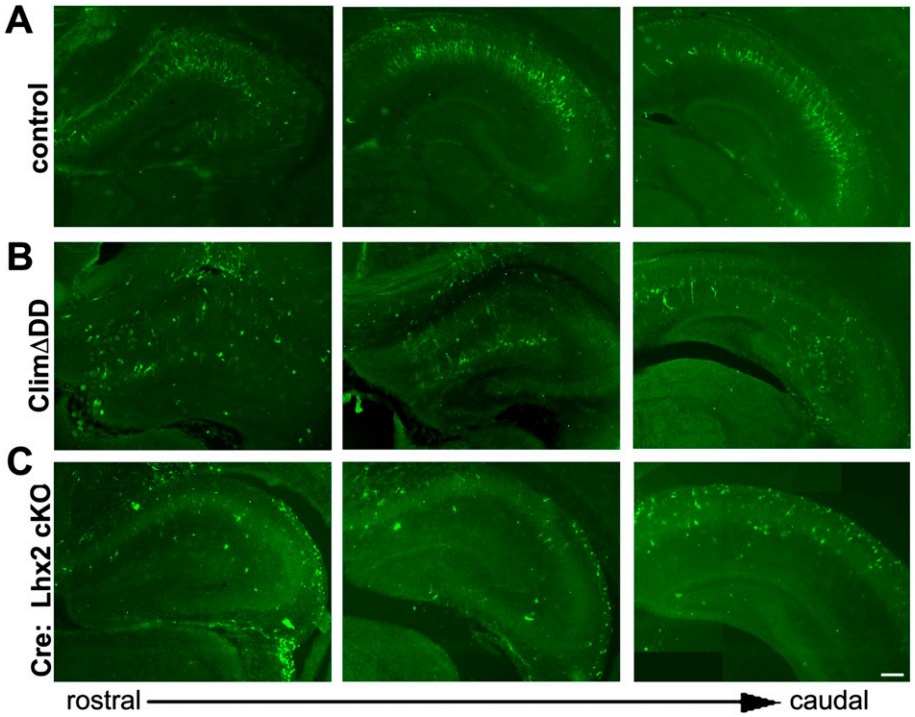

Fig. S2. Rostrocaudal levels of Cre or ClimΔDD electroporation produce similar phenotypes throughout the hippocampus. (*A*) Rostrocaudal series of sections from a WT embryo electroporated with a control GFP construct electroporated at E15 and examined 7 d later. Most of the labeled cells are seen in a tightly packed pyramidal cell layer. (*B*) Electroporation of *ClimΔDD* into WT embryos generates cells scattered throughout the hippocampus, which have multipolar morphologies. (*C*) This effect is seen at all rostrocaudal levels, similar to the phenotype seen when Cre is electroporated into *Lhx2* cKO embryos. *C* (third panel) is assembled from multiple epifluorescence images.

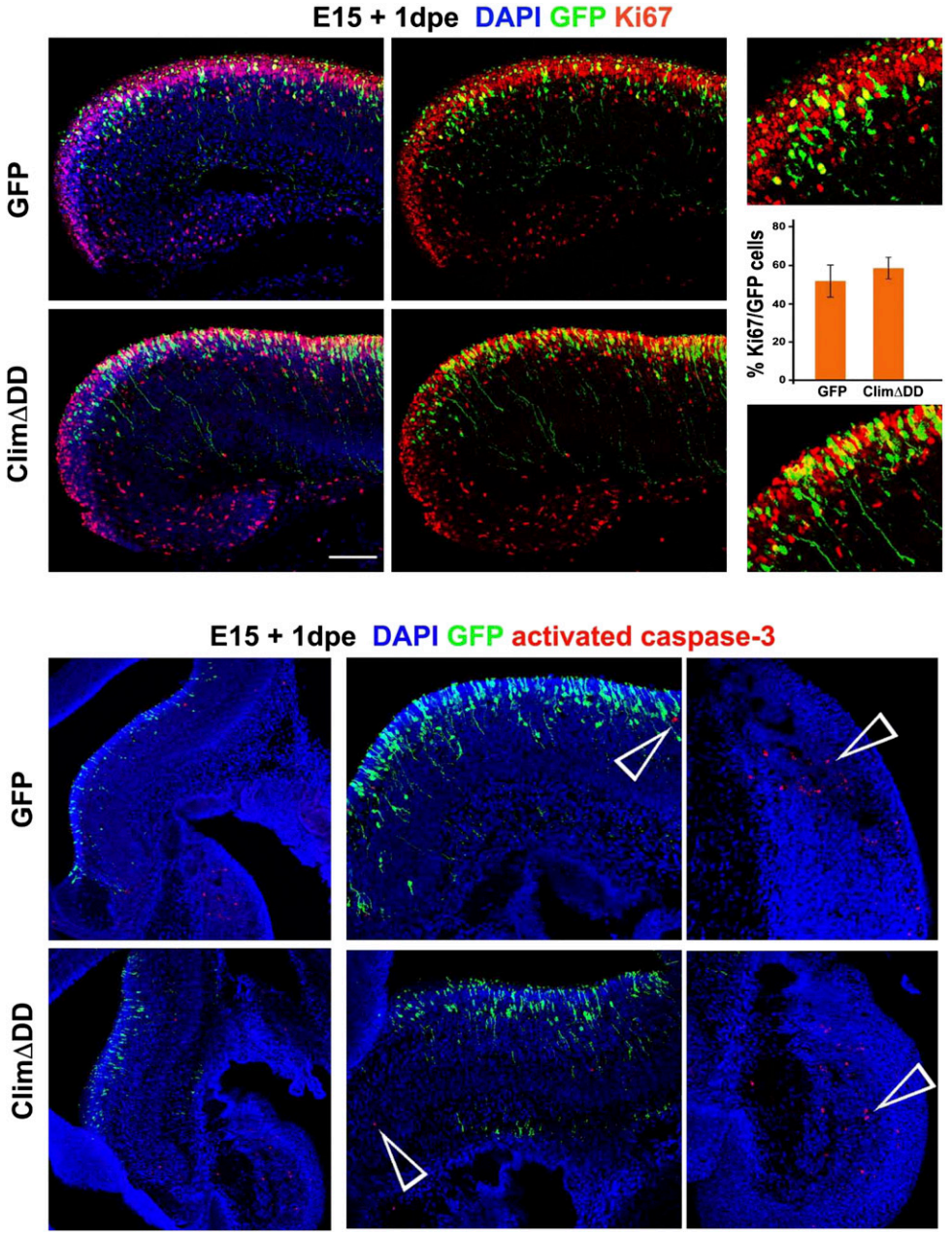

Fig. S3. ClimΔDD does not result in aberrant proliferation or cell death. E15 control GFP and ClimΔDD electroporated brains were examined 1 d after electroporation. dpe, days postelectroporation. Electroporated cells (green) were still at or near the ventricular zone, and similar proportions of these coexpressed proliferation marker Ki67 (red) in control (51.7%) and ClimΔDD (58.4%) electroporated brains (not significant; $P > 0.05$). The sections were counterstained with DAPI (blue). Similarly, staining for activated caspase 3 (red, arrowheads) did not show any enhanced cell death in the experimental brains. A few positive cells were detected in the adjacent portion of the thalamus of both control and ClimΔDD electroporated brains, providing an internal control for the activated caspase staining.

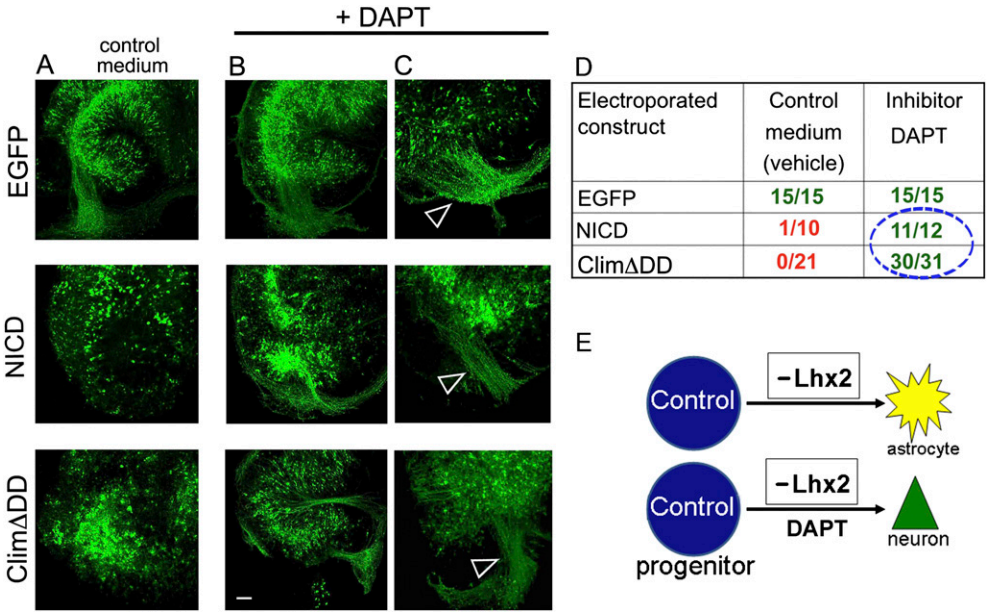

Electroporated construct	Control medium (vehicle)	Inhibitor DAPT
EGFP	15/15	15/15
NICD	1/10	11/12
ClimΔDD	0/21	30/31

Fig. S4. ClimΔDD does not cause astrogliogenesis if the Notch pathway is inhibited. (*A*) Organotypic explant cultures prepared at E15, electroporated with a control (GFP) construct, and examined 6 d later (+6 days in vitro) display robust axon bundles. Electroporation of either NICD or ClimΔDD switches the electroporated cells to an astrocytic fate, and axon bundles are no longer detectable. (*B* and *C*) Exposure to 1 μM DAPT on the first day of the 6-d culture period rescues neurogenesis in both NICD and ClimΔDD cultures and produces a phenotype indistinguishable from control GFP electroporations. The arrowhead marks the fimbria. (*D*) Tabluated results of the experiments shown in *A*–*C*. The number of explants with detectable axons was scored. (*E*) Diagram illustrating the results. Most images were assembled from two confocal images.

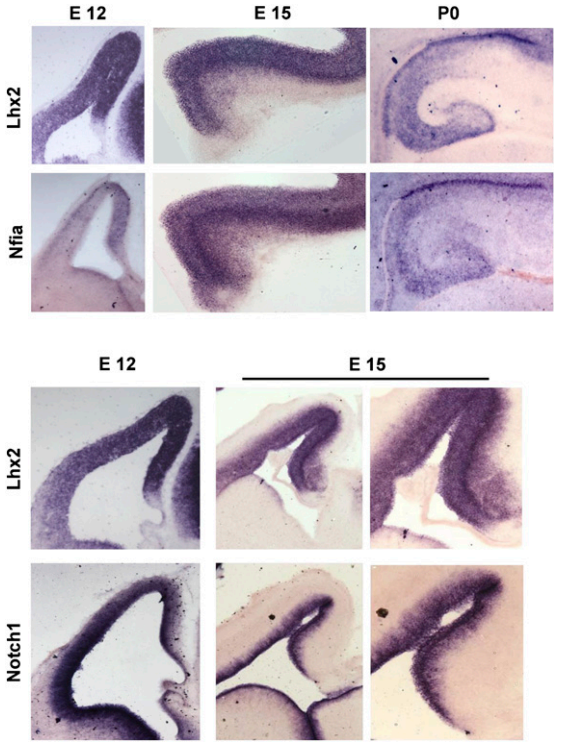

Fig. S5. *Lhx2*, *Notch1*, and *Nfia* expression across development. In situ hybridization in sections of E12, E15, and P0 brains display intense *Lhx2* expression intensely in the hippocampal ventricular zone at E12 and E15. This expression declines by P0. *Nfia* expression appears weakly detectable in the hippocampal ventricular zone at all these ages. *Notch1* is intensely expressed in the E12 and E15 brains in the hippocampal ventricular zone.

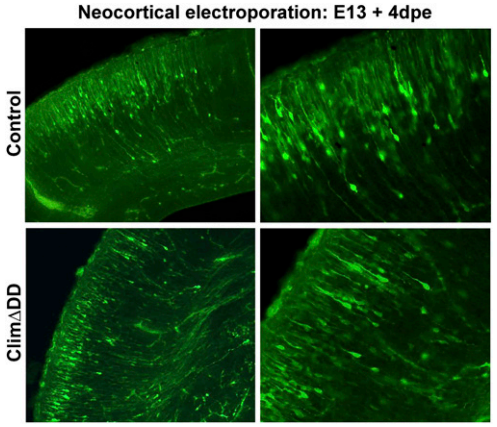

Fig. S6. Neocortical electroporation at E13, with either GFP or *ClimΔDD* construct, reveals cells with pyramidal neuron morphologies that have migrated to the cortical plate 4 d later. These cells display apical dendrites and extend axons that course through the intermediate zone. dpe, days postelectroporation.